Purinergic Signalling (2017) 13:545–557
DOI 10.1007/s11302-017-9582-3

ORIGINAL ARTICLE

Bone turnover is altered in transgenic rats overexpressing the P2Y2 purinergic receptor

Maria Ellegaard[1] · Cansu Agca[2] · Solveig Petersen[1] · Ankita Agrawal[1,3] · Lars Schack Kruse[1] · Ning Wang[3] · Alison Gartland[3] · Jens-Erik Beck Jensen[4] · Niklas Rye Jørgensen[1,5] · Yuksel Agca[2]

Received: 19 May 2017 / Accepted: 10 August 2017 / Published online: 21 August 2017

Abstract It is now widely recognized that purinergic signaling plays an important role in the regulation of bone remodeling. One receptor subtype, which has been suggested to be involved in this regulation, is the P2Y2 receptor (P2Y2R). In the present study, we investigated the effect of P2Y2R overexpression on bone status and bone cell function using a transgenic rat. Three-month-old female transgenic Sprague Dawley rats overexpressing P2Y2R (P2Y2R-Tg) showed higher bone strength of the femoral neck. Histomorphometry showed increase in resorptive surfaces and reduction in mineralizing surfaces. Both mineral apposition rate and thickness of the endocortical osteoid layer were higher in the P2Y2R-Tg rats. μCT analysis showed reduced trabecular thickness and structural model index in P2Y2R-Tg rats. Femoral length was increased in the P2Y2R-Tg rats compared to Wt rats. In vitro, there was an increased formation of osteoclasts, but no change in total resorption in cultures from P2Y2R-Tg rats. The formation of mineralized nodules was significantly reduced in the osteoblastic cultures from P2Y2R-Tg rats. In conclusion, our study suggests that P2Y2R is involved in regulation of bone turnover, due to the effects on both osteoblasts and osteoclasts and that these effects might be relevant in the regulation of bone growth.

Keywords Genetic animal models · Osteoblasts · Osteoclasts · Cell/tissue signaling · P2Y2 purinergic receptors

Maria Ellegaard and Cansu Agca are joint-first authors.

✉ Niklas Rye Jørgensen
Niklas@dadlnet.dk

✉ Yuksel Agca
agcay@missouri.edu

Maria Ellegaard
marlar04@regionh.dk

Cansu Agca
agcac@missouri.edu

Solveig Petersen
solpet02@regionh.dk

Ankita Agrawal
ankita2386@gmail.com

Lars Schack Kruse
lars.schack.kruse@regionh.dk

Ning Wang
n.wang@sheffield.ac.uk

Alison Gartland
a.gartland@sheffield.ac.uk

Jens-Erik Beck Jensen
jebj@dadlnet.dk

[1] Department of Clinical Biochemistry, Rigshospitalet, Copenhagen, Denmark

[2] College of Veterinary Medicine, University of Missouri, Columbia, MO, USA

[3] Mellanby Centre for Bone Research, University of Sheffield, Sheffield, UK

[4] Osteoporosis and Bone Metabolic Unit, Department of Endocrinology, Copenhagen University Hospital Hvidovre, Hvidovre, Denmark

[5] OPEN, Odense Patient data Explorative Network, Odense University Hospital/Institute of Clinical Research, University of Southern Denmark, Odense, Denmark

Introduction

Bone is a dynamic tissue which is constantly broken down and rebuilt. Imbalance between bone formation and resorption can eventually lead to the development of osteoporosis and subsequently an increased risk of fractures. It is therefore necessary that the balance between the activity of the bone-forming osteoblasts and the bone-resorbing osteoclasts is tightly regulated.

It is now widely recognized that purinergic signaling plays an important role in this regulation. Bone cells release nucleotides including adenosine triphosphate (ATP), adenosine diphosphate (ADP), uridine triphosphate (UTP), and uridine diphosphate (UDP) into the extracellular space. The targets for the extracellular nucleotides are the purinergic receptors. Differences in the molecular organization and signaling mechanisms divide purinergic receptors into two substantially different groups, namely, P2X and P2Y receptors [1]. Currently, seven P2X receptors and eight P2Y receptors have been identified and several of them have been shown to be expressed by one or more types of bone cells [2]. One receptor subtype, which has been suggested to play an important role in the regulation of bone remodeling, is the P2Y2 receptor (P2Y2R). P2Y2R has, besides ATP, also UTP as natural ligand, leading to both activation of phospholipase C β and generation of inositol 1,4,5-triphosphate, increasing intracellular calcium and activation of protein kinase C [3].

P2Y2R has been reported to be expressed by human and rat osteoblasts in culture [4, 5], where stimulation of the receptor induces c-Fos activation. Moreover, the response is strongly potentiated by parathyroid hormone pretreatment of the cells [4]. The expression of P2Y2R is dependent on the differentiation state of the osteoblasts, with more mature cells displaying an increased level of expression [6]. Stimulation of primary rat osteoblast cultures with ATP or UTP (1–100 μM) has been shown to inhibit mineralized bone nodule formation [7] by a mechanism not involving P2Y4R [6]. However, ATP and UTP (100 μM) have also been shown to increase mineralized bone nodule formation in primary rat osteoblasts, possibly through a mechanism involving upregulation of bone morphogenetic proteins (BMP) [8]. The expression of P2Y2R in osteoclasts is less clear. Bowler et al. reported that human osteoclasts express P2Y2R; however, resorptive activity of the cells was unaffected by UTP stimulation in contrast to ATP stimulation which increases their resorptive activity [9]. Furthermore, P2Y2R has been shown to be involved in intercellular communication between bone cells [10–12] and suggested to play a role in the mechanosensitivity of osteoblasts [13].

Studies on the in vivo effect of P2Y2R on bone turnover are very limited and have shown contrasting results. Whereas Orriss et al. found higher bone mineral content (BMC) in P2Y2R KO mice compared to wild-type (Wt) mice [7], Xing et al. found that P2Y2R KO mice had lower bone volume and bone strength than Wt mice [14].

More than 100 single-nucleotide polymorphisms (SNPs) have been reported within the human P2Y2R gene [15–17]. Recently, Wesselius et al. reported that the allelic versions of Leu46Pro polymorphism in the P2Y2R gene were associated with bone mineral density (BMD) of the lumbar spine, femoral neck, and total hip in a cohort of fracture patients, supporting a role for P2Y2R in the regulation of bone turnover and the risk of osteoporosis [18]. Furthermore, the Arg312Ser polymorphism has been shown to be associated with BMD in a study of postmenopausal women, where subjects homozygous for the variant allele displayed increased BMD and reduced bone loss [19].

Taken together, the research in the field suggests an important role for P2Y2R in bone biology; however, the exact involvement of the P2Y2R in regulation of bone turnover still remains unclear. In the present study, we investigated the effect of P2Y2R overexpression on bone status using a recently developed transgenic rat model. Furthermore, we investigated the underlying cellular effects of P2Y2R overexpression in primary osteoblasts and osteoclasts, in vitro.

Methods

In vivo study design

Nine female 3-month-old Sprague Dawley rats overexpressing P2Y2R (homozygous transgenic) and ten Wt Sprague Dawley rats were used in the study. Briefly, a lentiviral vector containing P2Y2R controlled by the ubiquitin promoter was microinjected into outbred Sprague Dawley zygotes, which were transferred into pseudopregnant Sprague Dawley recipient rats. Germline transgenic offspring were backcrossed for six generations to ensure stability of the transgene as described by Agca et al. [20]. Animals were fed by Purina, LabDiet®5008, and kept at 20 °C using a 14-h/10-h light-dark cycle. All animals received intraperitoneal injections of calcein (Sigma-Aldrich 20 mg/kg) 2 and 10 days before sacrifice in order to label a newly formed mineralized bone matrix. Blood was collected after euthanasia, and serum was stored at − 80 °C for subsequent measurements of bone resorption and formation markers. The left femur and tibia were stored in formalin for 48 h and thereafter transferred to 70% ethanol at 4 °C prior to μCT analysis. The right femur was cleaned of soft tissue, wrapped in saline-moistened gauze, and stored at − 20 °C for later ex vivo bone strength measurements, and the right tibia was isolated and stored in 70% ethanol at 4 °C for bone histomorphometric assessment. The length of the femur was measured in duplicate using a sliding caliper.

DXA measurements

Right femurs were scanned in duplicate on a PIXImus dual-energy X-ray (DXA) densitometer (Lunar Corporation, Madison, WI) to assess BMD, BMC, and bone area. The machine was calibrated daily with a phantom provided by the manufacturer.

MicroCT measurements

MicroCT analysis of trabecular bone microstructure was performed at the intact proximal tibia, with a resolution of 7.4 μm (SkyScan 1172 desktop μCT). The X-ray source was operated at 70 kV and 142 μA with a 0.5 aluminum filter. X-ray projection images were captured every 0.7° through 180° rotation of the bone and were then reconstructed by SkyScan NRecon software at a threshold (the scaling range from floating point to 8-bit integer values) of 0.0–0.10. SkyScan CTan software was then used to measure the structural parameters from a 4.0-mm thick trabecular abundant region of interest (ROI) 1.2 mm below the growth plate. Trabecular and cortical bone was separated by manually drawing around each compartment by a trained scientist and in accordance with published guidelines. The bone was identified using a global fixed threshold. This was determined empirically by visually comparing the raw scan and the thresholded scan to ensure accuracy. Using a global fixed threshold (as opposed to a specimen-specific or local segmentation method) ensures that differences between study groups are due to experimental effects rather than image processing effects. The following indices were determined: trabecular bone volume fraction (BV/TV, %), trabecular thickness (Tb.Th, μm), trabecular number (Tb.N, 1/mm), trabecular separation (Tb.Sp, mm), trabecular pattern factor (Tb.Pf, 1/mm), structure model index (SMI), trabecular BMD, cortical thickness (Ct.Th.), cortical bone volume (BV), cortical porosity, and cortical BMD.

Bone strength measurements

Ex vivo biomechanical bone strength measurements were performed as described earlier [21]. In short, the femoral diaphysis was subjected to a three-point bending test and the femoral neck was subjected to shear test on a Lloyd material testing device LR50K (Lloyd Instruments, Fareham, UK). Testing of biomechanical properties was performed after rehydration in a saline solution at room temperature overnight. For the three-point bending test, the femur was placed horizontally on two supports (distance 18 mm) with deflection of the midshaft using a vertical probe with a constant speed of 2 mm per minute and a 500 N load cell. Load-displacement curves were generated and a maximum load applied until fracture was recorded, stiffness was calculated as the slope of the linear part of the curve, and work-to-failure was calculated as area under the curve.

Bone turnover markers

Bone turnover markers in serum samples were analyzed in duplicate following the instructions supplied by the manufacturer (Rat-MID Osteocalcin EIA, RatLaps (CTX-I), procollagen type 1, N-terminal (P1NP), and RatTRAP (IDS, DK)). To determine alkaline phosphatase (ALP) activity, the substrate solution was prepared by dissolving *p*-nitrophenyl-phosphate tablet (Sigma-Aldrich) in an assay buffer (Sigma-Aldrich), and the *p*-nitrophenol standard dilution was made in the assay buffer. Prediluted serum samples, control, or standards were assayed in duplicate at 37 °C for 30 min, and the reaction was terminated with 1 M NaOH. The absorbance was read at 405 nm by an ELISA reader (Infinite M200 Magellan, Tecan).

Bone histomorphometry

Histomorphometric analyses were performed as previously described [22]. In short, the bones were dehydrated in a graded series of ethanol solutions and embedded in methyl methacrylate. The bones were sectioned longitudinally through the frontal plane (7 μm thick) using a Polycut E microtome and a tungsten carbide knife. Sections were mounted on gelatin-coated slides and dried for 1 h at 40 °C before further treatment. Five sections from each tibia were stained with Goldner's trichrome, and five sections were left unstained for analysis of fluorochrome labels. Sections were analyzed using an Olympus BX51 microscope attached to an image analyzer (C.A.S.T. GRID system from Olympus Denmark 2000). The following indices were measured in the proximal tibia: osteoid thickness (O.Th, μm), cortical thickness (Ct.Th, μm), percentage of eroded surface (ES/BS, %), percentage of mineralizing surfaces (MS/BS, %), and mineral apposition rate (MAR).

Osteoblast isolation

Primary rat calvarial osteoblasts were isolated from P2Y2R Tg and Wt rats as described by Orriss et al. [23]. In short, calvariae from 2- to 3-day-old rat pups were removed in sterile surroundings and cleaned from excess tissue and cartilage. The calvariae were washed with PBS, treated with trypsin, before sequential collagenase digestion (0.2% collagenase type II (Sigma-Aldrich) in Hanks' Balanced Salt Solution (HBSS, Invitrogen)). The final cell fraction was washed by centrifugation, resuspended in DMEM containing 10% FBS, 100 μg/ml penicillin and streptomycin (P/S, Invitrogen), and 2 mM Glutamax (Invitrogen), pH = 7.4), and seeded in 80 cm^2 flasks. Cells were incubated for 2–3 h and washed again to

remove the non-adherent cells. Cells were cultured at 37 °C and 5% CO_2 until confluence (3–4 days), at which point they were seeded for experiments.

Osteoclast generation

Osteoclasts were generated from the bone marrow of P2Y2R Tg and Wt rats. The mononuclear fraction of non-adherent cells from the bone marrow was isolated on a Histopaque-1077 gradient and then collected after a 10-min centrifugation at 400×*g*. They were then resuspended in α-MEM (containing 10% FCS, P/S, 2 mM L-glutamine, 60 ng/ml macrophage colony-stimulating factor (M-CSF), pH = 7.35–7.4). The suspensions were seeded in a six-well plate at a concentration of 1.5×10^7 cells per well. After 1 day of culture, non-adherent cells were removed, and each well was washed twice with culture medium before addition of M-CSF and receptor activator of nuclear factor kappa-B ligand (RANKL) to the cultures (30 ng M-CSF/ml, 40 ng RANKL/ml).

Calcium assay

Cells were seeded in triplicates at a density of 10.000/well in a 96-well plate (black with transparent bottom). After 24 h of culture, the wells were washed once in Ca buffer (HBSS (+/+) with 10 mM Hepes and 2 mM probenecid, pH 7.4) and then incubated at 37 °C for 30 min with Fluo-4 (50 μl/well of 1:1 2 mM Fluo-4 with 20% Pluronic F-127 in Ca buffer). Plates were then washed twice in Ca buffer and left in Ca buffer for 10 min at 37 °C before assay. Wells were then treated in triplicate with varying doses of agonist (UTP or ATP dissolved in dH_2O) and Ca release measured by Fluo-4 fluorescence using a NOVOstar detection unit in two steps: step 1 in five intervals of 0.3 s to establish baseline prior to agonist addition and then every 0.4 s in 150 intervals from 9 to 69 s to record agonist response. Wells without Flou-4 treatment (replaced by Ca buffer) acted as blank controls and were automatically subtracted from all results.

Quantitative polymerase chain reaction

Total RNA was isolated according to the manufacturer's recommendations including genomic DNA wipeout (Qiagen RNeasy Plus Universal Kit) from three Wt and three P2Y2R-Tg rats (6 and 8 weeks old, respectively) for lung and brain analysis and from calvarial osteoblasts in passage 1 isolated from 4- to 7-day-old rat pups ($n = 6$ for Wt and $n = 4$ for P2Y2R-Tg). Total RNA content was measured using a NanoDrop 2000 spectrophotometer. Reverse transcription was performed on a GeneAmp 9700 using the Applied Biosystems High-Capacity Reverse Transcription Kit according to the manufacturer's recommendations with 100 ng total RNA as input per complementary DNA (cDNA) reaction. Settings were 25 °C for 10 min, then 37 °C for 120 min, then 85 °C for 5 min, and finally 4 °C until use or storage.

qPCR was performed using a 2-μl cDNA template and the Applied Biosystems TaqMan© Universal PCR Master Mix plus relevant TaqMan probes (rat P2Y2, #Rn02070661_s1, and rat HPRT1, Rn01527840_m1) according to the manufacturer's recommendations in 20 μl total volume. All samples were run in triplicate, on a QuantFlex7 unit using the "standard curve" program. Data were analyzed using the comparative ΔΔCt method and expressed as fold change compared to wild-type levels.

Western blotting

Tissue sections and cultured cells were mixed with lysis buffer containing protease and phosphatase inhibitors (Roche) and disrupted and homogenized by sonication. The resulting homogenates were precleared of cellular debris by centrifugation at 11.000×*g* for 15 min at 4C. Total protein content of the supernatants was measured by the Bio-Rad DC total protein content kit according to the manufacturer's recommendations.

Samples were prepared by adjusting total protein content to 20 μg/loading in LDS buffer (Expedeon) with 50 mM DTT (AppliChem). Samples were run on 4–20% TGX gradient gels (Bio-Rad) for 35 min at 200 V and 110 mA/gel. Proteins were immediately electroblotted onto 0.2-μm PVDF membranes using a Bio-Rad Trans-Blot Turbo unit for 10 min set at the high MW protocol (1.3 A). The resulting membranes were blocked for 1 h at RT on an orbital shaker using 2% ECL Blocking Agent (GE Healthcare) in TBS-T (blocking buffer). They were incubated overnight using rabbit anti-P2Y2 (APR-010, Alomone Labs, 1:1000) or monoclonal rabbit anti-histone H3 (#4499S, Cell Signaling, 1:1000) in blocking buffer at 4 °C on a rotor; briefly washed twice in TBS-T and then incubated with HRP-conjugated donkey anti-rabbit IgG antibody (#NA934V, GE Healthcare, 1:40.000 in blocking buffer) at RT on a rotor; washed in large volumes of TBS-T; and finally developed using ECL Select Western Blotting Detection Kit (GE Healthcare) for 5 min at RT. Image capture by LAS-4000 and densiometric quantification were performed using Image Gauge 3.0 (Fujifilm) software where P2Y2 band intensity was normalized to histone H3 intensity and then presented relative to WT.

Osteoblast numbers and mineralization assay

Osteoblasts were grown in mineralization medium (DMEM, 50 μl/ml L-ascorbic acid phosphate (Wako Chemicals USA, Inc.), 2 mM β-glycerophosphate (Sigma-Aldrich)) for 7 days with media changed every 2 days.

Cell numbers were estimated by WST-1 assay, measuring mitochondrial activity. Medium was removed after 7 days, and experimental medium containing 10% WST-1 reagent

(Roche) was added. The plates were incubated at 37 °C with 5% CO_2 for 1 h, and 100 μl medium from each well was transferred to a 96-well ELISA plate (Nunc). The plates were read at 450 and 650 nm (as reference) by an ELISA reader (Infinite M299 Magellan, Tecan). Wells containing the WST-1 medium without cells were used as blanks and were subtracted from all measurements. Afterwards, WST-1 medium was removed and cells were fixated in ice-cold 70% ethanol for 1 h at 4 °C for mineralization assay. The wells were washed with distilled water, and cells were stained with 40 mM Alizarin Red S (AR-S) (Sigma-Aldrich), at pH 4.2 for 10 min at room temperature with shaking rotation at 2 g. The wells were washed three times with distilled water and finally washed with PBS with Ca^{2+} and Mg^{2+} for 15 min at room temperature with shaking rotation at 2 g to reduce non-specific AR-S staining. Cells were de-stained in 10% CPC (Sigma-Aldrich) for 15 min at room temperature with rotation at 2 g. Standard row dilutions and AR-S extracts were applied (100 μl/well in duplicate) into a 96-well ELISA plate, and AR-S concentration was determined on an ELISA reader (absorbance at 450 and 650 nm as reference). AR-S concentrations were normalized to cell number (estimated by WST-1 assay).

Measurement of collagen production

Collagen production was determined in osteoblast cultures after 14 days of culture in medium containing 5% fetal calf serum, 2 mM β-glycerophosphate, and 50 μg/ml L-ascorbic acid phosphate. To measure deposited (fibrillar) collagen, cultures were washed in PBS, fixed with Bouin's solution for 1 h, and washed extensively in running water. Plates were left to air dry before staining for 1 h with Sirius Red dye reagent (1 mg/ml Direct 80 in picric acid, Sigma-Aldrich) with gentle agitation. Plates were washed extensively with running water, followed by 0.01 M hydrochloric acid to remove unbound dye. The stained collagen layers were digested with 0.1 M sodium hydroxide (500 μl/well) for 30 min. The absorbance of the digests was measured at 570 nm by an ELISA reader.

Determination of ALP activity

The ALP activity of cell lysates was determined colorimetrically by an ELISA reader using a commercially available kit (Sigma-Aldrich) as described previously [24]. Osteoblasts were cultured in 24-well trays for 14 days. Cell layers were washed, and cells were harvested using a cell scraper followed by sonication at 4 °C and centrifugation at 500×*g*. The supernatant was collected and stored at − 18 °C. The cell lysate was diluted 25 times in TBS buffer. Total protein content was determined by Pierce BCA Protein Assay (Thermo Scientific). Cell lysate was thawed, and 50 μl lysate, control, or standard was transferred to a 96-well plate in duplicate. Two hundred microliters of working reagent was added to the each well before incubation for 60 min at 37 °C. The absorbance was read at 562 nm.

Resorption assay

Osteoclasts were isolated and cultured as described above but seeded in 96-well plates on bovine bone slices (Nordic Bioscience, Herlev, Denmark) or 48-well glass cover slips. After 10 days of culture, the osteoclasts on glass cover slips were stained for tartrate-resistant acid phosphatase (TRAP) and quantified by visible inspection of ten randomly chosen fields of view. Only TRAP-positive cells with more than three nuclei were counted as multinucleated osteoclasts. Cells were removed from the bone slices, and the resorption pits were stained with hematoxylin, prior to quantification with the C.A.S.T. (Computer Assisted Stereological Toolbox) Grid system on Olympus Bx51. The results were calculated as area resorbed in percentage of total area.

Approvals

Animals were housed in accordance with the policies of the University of Missouri Animal Care and Use Committee, and the Guide for the Care and Use of Laboratory Animals (protocol: 6466).

Statistics

Statistical analyses were performed using the SPSS software, v.11.5. For the comparison of the different genotypes, Student's *t* test was used for normally distributed data; otherwise, the non-parametric Mann-Whitney *U* test was used. Differences were considered statistically significant when $p \leq 0.05$. Normally distributed data are presented as mean ± standard error of the mean (SEM). Non-parametric data are presented as individual experiments and mean.

Results

P2Y2R overexpression increases femoral length but has no effect on bone mineral density

Femoral length was significantly higher in P2Y2R-Tg rats compared to Wt rats (3.52 ± 0.02 vs. 3.46 ± 0.01 cm, respectively; $p = 0.002$); however, there was no effect of P2Y2R overexpression on BMD, BMC, and bone area of the total femur determined by DXA (Table 1). μCT analysis confirmed these findings, showing no significant difference in either cortical or trabecular BMD between the genotypes (Table 2).

Table 1 Femoral DXA parameters and femoral length

	WT (mean ± SEM)	P2Y2R-Tg (mean ± SEM)	*p* value (*n* = 9–10)
BMD (g/cm^2)	0.1848 ± 0.0027	0.1839 ± 0.0033	0.846
BMC (g)	0.4015 ± 0.0092	0.4085 ± 0.0070	0.557
Bone area (cm^2)	2.17 ± 0.04	2.22 ± 0.04	0.364
Length (cm)	3.46 ± 0.01	3.52 ± 0.02	**0.002**

Statistically significant *p*-values are shown in bold.

P2Y2R overexpression changes the trabecular microstructure while cortical microstructure is unaffected

Microstructural analysis using μCT scan of the proximal tibia revealed a minor, but significant, decrease in Tb.Th in P2Y2R-Tg rats compared to Wt rats (0.0576 ± 0.0005 vs. 0.0592 ± 0.0005 mm, respectively, $p = 0.018$) (Table 2). SMI, which is used to measure the change in surface curvature in trabecular bone, was increased from 1.23 ± 0.081 in Wt rats to 1.46 ± 0.045 in P2Y2R-Tg rats ($p = 0.027$), indicating a more rod-like trabecular structure in P2Y2R-Tg rats (Table 2). There were no significant differences between genotypes in the other indices of the trabecular compartment (BV/TV, Tb.N, Tb.Sp Tb.PF) (Table 2). Furthermore, there were no significant differences in cortical microstructure (BV, Ct.Th, or porosity) between the genotypes (Table 2).

P2Y2R overexpression increases the strength of the femoral neck

Bone strength of the femoral neck was determined by shear test and revealed a significant 17% increase in maximum load of the femoral neck in P2Y2R-Tg rats compared to Wt rats ($p = 0.04$) (Table 3). There were no significant differences in stiffness or work-to-failure of the femoral neck between the genotypes, although the same trend was seen as for the maximum load (Table 3). Bone strength of the femoral midshaft was determined by the three-point bending test. There were no significant differences in maximum load, stiffness, or work-to-failure of the femoral midshaft between the genotypes (Table 3).

P2Y2R overexpression affects both bone resorption and bone formation

Histomorphometric analysis of the proximal tibia demonstrated significant effects of P2Y2R overexpression. ES/BS was significantly higher in P2Y2R-Tg rats compared to Wt rats (18.9 ± 0.5 vs. 16.9 ± 0.5%, respectively; $p = 0.010$) (Table 4). MS/BS was decreased by 6% in P2Y2R-Tg rats compared to Wt rats ($p = 0.008$); however, MAR was increased by 10% in P2Y2R-Tg rats compared to Wt rats ($p = 0.032$), but no difference in BFR/BS was seen (Table 4). To assess the apposition of the unmineralized bone matrix, endosteal O.Th in the proximal tibia adjacent to the growth plate was measured. O.Th was significantly increased by 41% in P2Y2R-Tg rats compared to Wt rats ($p < 0.001$) (Table 4 and Fig. 1). In contrast, no osteoid tissue was found in the trabecular compartment, nor in the cortical bone in the diaphysis.

Table 2 Trabecular and cortical microstructural parameters determined by μCT

	WT (mean ± SEM)	P2Y2R-Tg (mean ± SEM)	*p* value (*n* = 9–10)
Trabecular bone			
BMD (g/cm^3)	0.897 ± 0.004	0.898 ± 0.003	0.737
BV/TV (%)	20.7 ± 1.2	19.8 ± 0.5	0.512
Tb.Th (mm)	0.0592 ± 0.0005	0.0576 ± 0.0005	**0.018**
Tb.N (1/mm)	3.49 ± 0.20	3.44 ± 0.09	0.827
Tb.Sp (mm)	0.177 ± 0.008	0.170 ± 0.005	0.509
Tb.Pf (1/mm)	6.02 ± 1.59	9.38 ± 0.73	0.079
SMI (−)	1.23 ± 0.08	1.46 ± 0.05	**0.027**
Cortical bone			
BMD (g/cm^3)	1.234 ± 0.010	1.253 ± 0.009	0.180
BV (mm^3)	4.51 ± 0.05	4.64 ± 0.07	0.166
Porosity (−)	1.02 ± 0.07	0.91 ± 0.05	0.246
Ct.Th (mm)	0.394 ± 0.006	0.406 ± 0.007	0.191

Statistically significant *p*-values are shown in bold.

Table 3 Biomechanical bone strength parameters

	WT (mean ± SEM)	P2Y2R-Tg (mean ± SEM)	*p* value (*n*)
Femoral midshaft			
Maximum load (N)	100.0 ± 2,1	99.3 ± 2.9	0.862 (9–10)
Stiffness (N/mm)	247.7 ± 7.3	260.7 ± 11.1	0.333 (9–10)
Work to failure (N*mm)	57.0 ± 3.1	49.1 ± 2.9	0.078 (9–10)
Femoral neck			
Maximum load (N)	61.1 ± 3.9	71.6 ± 2.8	**0.040 (8–9)**
Stiffness (N/mm)	73.2 ± 2.8	81.9 ± 4.2	0.114 (8–9)
Work to failure (N*mm)	30.4 ± 2.5	38.8 ± 3.6	0.081 (8–9)

Statistically significant *p*-values are shown in bold.

In accordance with the histomorphometry, serum bone resorption marker TRAP-5b was significantly higher in P2Y2R-Tg rats compared to Wt rats (2.08 ± 0.17 vs. 1.50 ± 0.09 U/l, respectively; $p = 0.006$) (Table 5). There was, however, no difference in resorption marker CTX-I between the genotypes (Table 5). No significant differences between genotypes could be detected in the bone formation markers, osteocalcin, and P1NP, while ALP activity in serum was 25% lower in P2Y2R-Tg rats compared to Wt rats ($p = 0.001$) (Table 5).

P2Y2R is greatly overexpressed in some tissues from the P2Y2R-Tg rat

To demonstrate to which extent cells and tissues from P2Y2R-Tg rats overexpress messenger RNA (mRNA) for P2Y2R, brain and lungs were isolated for qPCR. In the brain and lungs, we found that P2Y2R expression increased 300-fold (range 241–407) and 120-fold (range 118–128), respectively, for the P2Y2R-Tg rat compared to WT. In osteoblasts isolated from calvariae of the transgenic animals, P2Y2R mRNA expression was increased by almost 90-fold (range 81–104) (Fig. 2a).

To determine the effect on the expression of the P2Y2R protein, Western blotting was performed. While total P2Y2R protein expression (basal and glycosylated) in the brain was increased by 67 ± 12% ($p = 0.010$), no increased P2Y2R protein expression could be detected in the calvarial osteoblast cultures from P2Y2R-Tg rats (90 ± 18% of WT_{mean}, $p = 0.70$) (Fig. 2b).

P2Y2R overexpression increases the intracellular calcium response to nucleotides

In order to determine whether the increased P2Y2R expression translated into a cellular phenotype, the intracellular calcium response to UTP stimulation was investigated in cultures of calvarial osteoblasts. The increase in intracellular calcium concentration upon UTP stimulation was significantly higher in osteoblasts from P2Y2R-Tg compared to the cells obtained from WT animals ($p < 0.0001$) (Fig. 3).

P2Y2R overexpression affects osteoclast formation and activity in vitro

By days 3–4 of culture, TRAP-positive mononuclear cells appeared and multinucleated cells after a week. The number of TRAP-positive multinucleated cells reached a maximum on day 12. The number of osteoclasts formed after 10 days of culture was significantly higher in P2Y2R-Tg rats compared to Wt rats (568 ± 47 vs. 433 ± 34, respectively; $p = 0.032$) (Fig. 4a). In contrast, there was a trend towards decreased resorbed area of osteoclasts from P2Y2R-Tg rats compared to Wt rats; however, it did not reach statistical significance (41.7 ± 2.68 vs. 54.1 ± 5.30%, respectively; $p = 0.056$) (Fig. 4b).

Table 4 Histomorphometry of the proximal tibia in P2Y2R-Tg and Wt rats

	WT (mean ± SEM)	P2Y2R-Tg (mean ± SEM)	*p* value (*n*)
ES/BS (%)	16.9 ± 0.5	18.9 ± 0.5	**0.010 (9–10)**
MS/BS (%)	60.6 ± 1.0	56.9 ± 0.5	**0.008 (9–10)**
MAR μm/day	0.94 ± 0.02	1.03 ± 0.03	**0.032 (9–10)**
BFR/BS (μm/day)	56.9 ± 1.5	58.6 ± 1.8	0.536 (8–10)
O.Th (μm)	11.0 ± 0.5	15.5 ± 0.6	**< 0.001 (9–10)**

Statistically significant *p*-values are shown in bold.

ES/BS eroded surfaces, *MS/BS* mineralized surfaces, *MAR* mineral apposition rate, *BFR/BS* bone formation rate, *O.Th* osteoid thickness

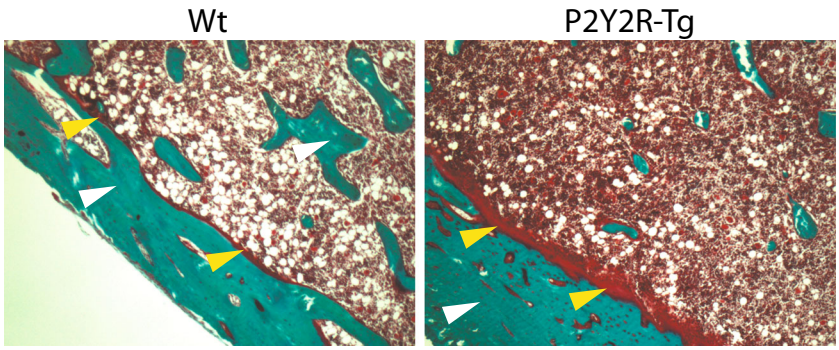

Fig. 1 Micrograph of osteoid formation determined on Goldner's trichrome-stained bone sections of the cortical bone of the tibia from P2Y2R-Tg rats and Wt rats (*white arrow*: bone; *yellow arrow*: osteoid)

P2Y2R overexpression reduces mineralization in primary rat osteoblastic cell cultures

In vitro, primary osteoblastic cells from P2Y2R-Tg rats showed reduced formation of mineralized bone nodules at day 7 ($p = 0.021$) (Fig. 5a). While there was no significant difference in collagen production (Fig. 5b), the ALP activity was decreased by 40% in osteoblasts from P2Y2R-Tg rats compared to osteoblasts from Wt rats ($p = 0.004$) (Fig. 5c).

Discussion

In summary, 3-month-old female rats overexpressing P2Y2R showed higher bone strength of the femoral neck. Histomorphometric analysis showed increased number of resorptive surfaces and MS/BS was reduced. However, there was an increase in both MAR and O.Th. μCT analysis showed a minor reduction in trabecular thickness and a slight change in SMI pointing to a more rod-like structure in P2Y2R-Tg rats. The effect of P2Y2R overexpression did not result in an overall change in BMD, BMC, or bone area, although length growth was slightly increased compared to Wt rats. In vitro, there was an increased formation of osteoclasts from the transgenic rats, but no change in total resorption, while the formation of mineralized nodules was significantly reduced in the osteoblastic cultures from P2Y2R-Tg rats.

Prior published studies on the involvement of ATP, UTP, and P2Y2R in bone turnover have shown somewhat contradictory results. Until now, the effect of P2Y2R signaling on bone status in vivo has been sparsely investigated and limited to the use of P2Y2R KO mice, due to the limited P2Y2R-specific agonists and antagonists. This led us to investigate whether increased P2Y2R expression in vivo was associated with a change in bone status using a novel P2Y2R-overexpressing transgenic rat strain. This model was developed by Agca et al. and has been shown to express increased levels of functional P2Y2R in various tissues [20]. However, as the original report on the transgenic model did not address P2Y2R expression in bone and bone cells, we investigated P2Y2R expression in cultured calvarial osteoblasts from the P2Y2R-Tg and WT rats. We found a substantial overexpression of the receptor by qPCR. However, we were unable to demonstrate an upregulation of the receptor protein. This could be explained with missing translation of mRNA expression into P2Y2R proteins. Interestingly, we still found an increased dose-dependent response of the cells to UTP stimulation, indicating that at least some of the increased mRNAs is translated into membrane-bound P2Y2R, as the intracellular calcium increase was enhanced by approximately 50–70% in cells from P2Y2R-Tg rats when compared to cells from Wt rats. This is similar to what was shown in smooth muscle cells in the original report on the phenotype of the P2Y2R-Tg model. This discrepancy between increase in mRNA expression of the receptor and yet no detectable increase in protein levels of

Table 5 Serum bone turnover markers

	WT (mean ± SEM)	P2Y2R-Tg (mean ± SEM)	*p* value (*n*)
Resorption			
CTX-I (ng/ml)	36.0 ± 1.8	34.0 ± 1.7	0.448 (9–10)
TRAP5b (U/l)	1.50 ± 0.09	2.08 ± 0.17	**0.006 (9–10)**
Formation			
Osteocalcin (ng/ml)	199.9 ± 16.6	184.5 ± 11.2	0.463 (9–10)
PINP (ng/ml)	1.86 ± 0.14	1.54 ± 0.11	0.113 (8–10)
ALP (nmol/ml)	95.79 ± 3.39	72.32 ± 5.02	**0.001 (9–10)**

Statistically significant *p*-values are shown in bold.

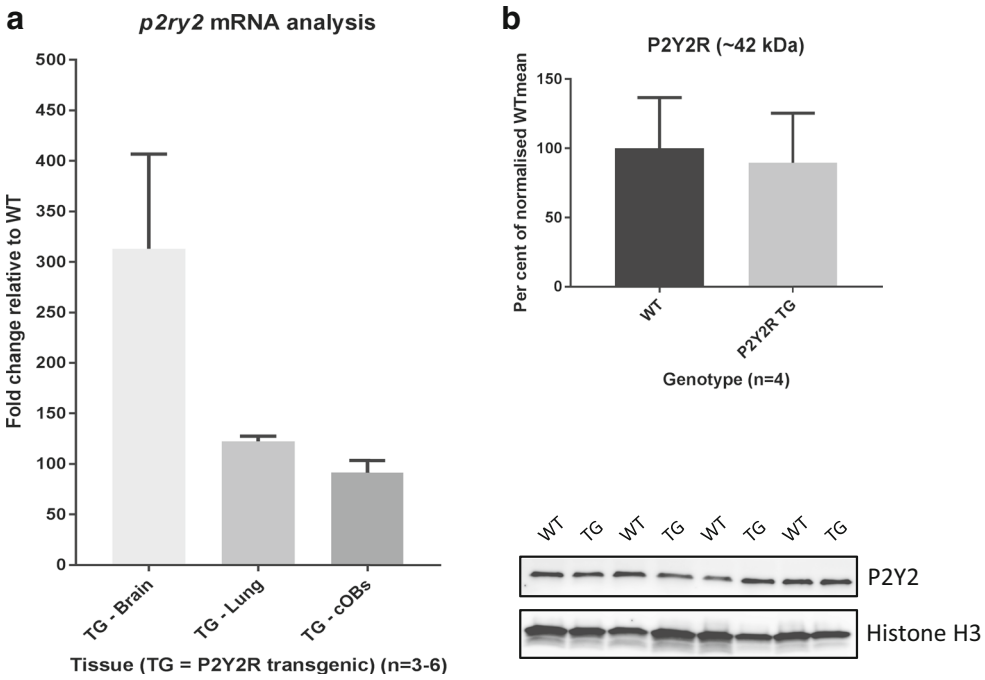

Fig. 2 **a** Fold change in expression of P2Y2 mRNA in brain and lung tissue ($n = 3$) as well as calvarial osteoblasts ($n = 4$) of P2Y2R-Tg rats relative to Wt ($n = 3$ (brain and lung); $n = 6$ (calvarial osteoblasts)). **b** P2Y2R protein expression in calvarial osteoblasts from WT ($n = 4$) and P2Y2R-Tg ($n = 4$) rats as measured by Western blotting. All bands are normalized to histone H3 expression, and mean expression in Wt cells is set at 100%. *Lower panel* shows membrane images of each individual experiment. *Error bars* represent SEM. *TG* P2Y2R transgenic, *Wt* wild-type

the receptor may occur if the massive increase in mRNA in the transgenic animals leads to prolonged surface expression, thus giving rise to an increase in receptor signaling. Alternatively, the distribution of receptors between the intracellular compartment and the cell membrane could be changed as a result of the increased transcript levels. However, as we did not examine the membrane-to-cytosol distribution and only measured total cellular P2Y2R protein content by Western blotting, we were unable to investigate this.

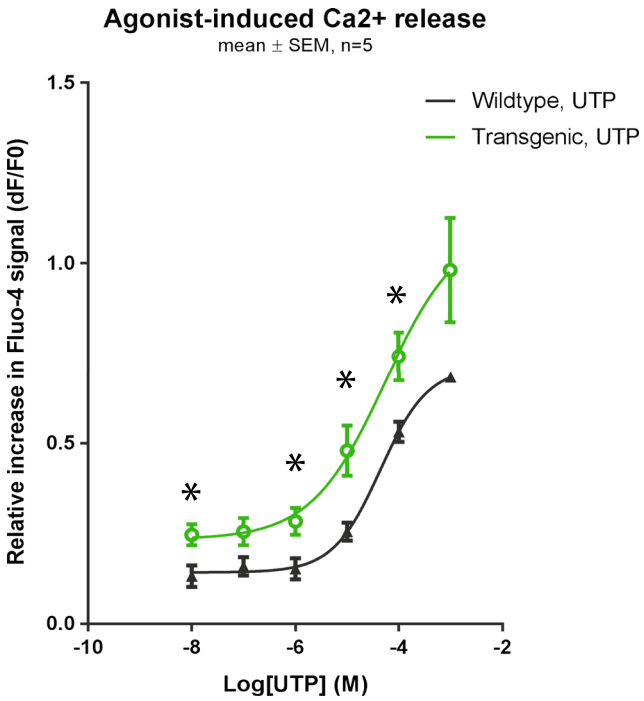

Fig. 3 Mean change in background subtracted Fluo-4 fluorescence ± SEM as a measure of intracellular Ca2+ release for both Wt and P2Y2R-Tg rat calvarial osteoblasts ($n = 5$) using UTP as agonist. *$p < 0.05$

Moreover, we detected a bone phenotype in the P2Y2R-Tg animals. The trabecular region of the tibia showed thinning and a slightly more rod-like structure in P2Y2R-Tg rats. However, there were no differences in trabecular bone volume, number, or spacing of the trabeculae, suggesting that the effect on trabecular microstructure was limited. This was supported by the fact that mechanical bone strength parameters of the femoral neck—a region rich in trabecular bone—were not reduced. In contrast, we saw a 17% increase in maximum load of the femoral neck. Additionally, P2Y2R-Tg rats had longer femurs than Wt rats. This change in length growth, resulting in either larger bones or a change in bone geometry, may have contributed to the increased bone strength of the femoral neck in P2Y2R-Tg rats.

There was no effect of P2Y2R overexpression on cortical microstructure assessed by μCT, and in agreement with this, there was no change in mechanical strength parameters of the femoral midshaft, consisting primarily of cortical bone or in the total femoral BMD measured by DXA. Due to the relatively lower bone turnover in cortical bone compared to trabecular bone [25], a change in bone turnover would be expected to affect trabecular bone to a greater extent and at an earlier time point than cortical bone.

Histormophometric analysis revealed an 11% increase in resorption of trabecular bone surfaces in P2Y2R-Tg rats,

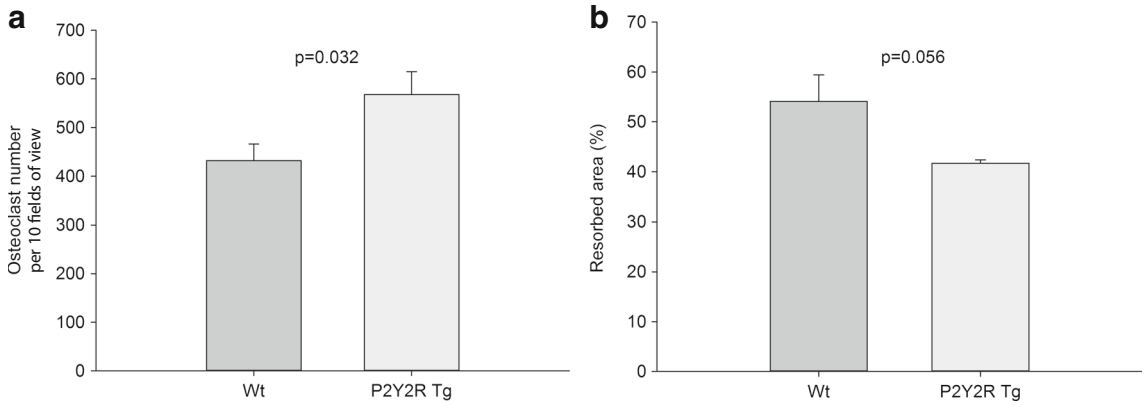

Fig. 4 **a** The total number of osteoclasts identified as TRAP-positive cells with three or more nuclei, developed from bone marrow from P2Y2R-Tg or Wt rats in ten randomly selected fields of view. **b** Resorption of bone slices by primary osteoclasts from P2Y2R-Tg or Wt rats (percentage of total area). Data are presented as mean ± SEM and *p* value from *t* test ($n = 10$)

suggesting a higher activation frequency. This was supported by the profound increase in the serum resorption marker TRAP5, which is related to the number of osteoclasts. There was, however, no change in the serum marker CTX-I—a product of collagenous matrix degradation. This could suggest that although more resorption sites appeared, the resorption depth might have been decreased in P2Y2R-Tg rats. Unfortunately, we did not measure this parameter. In accordance to this, P2Y2R-Tg rats showed an increased formation of multinucleated osteoclast-like cells in vitro, but no significant change in total resorbed area of bone slices compared to the primary osteoclasts from Wt rats. In fact, there was a

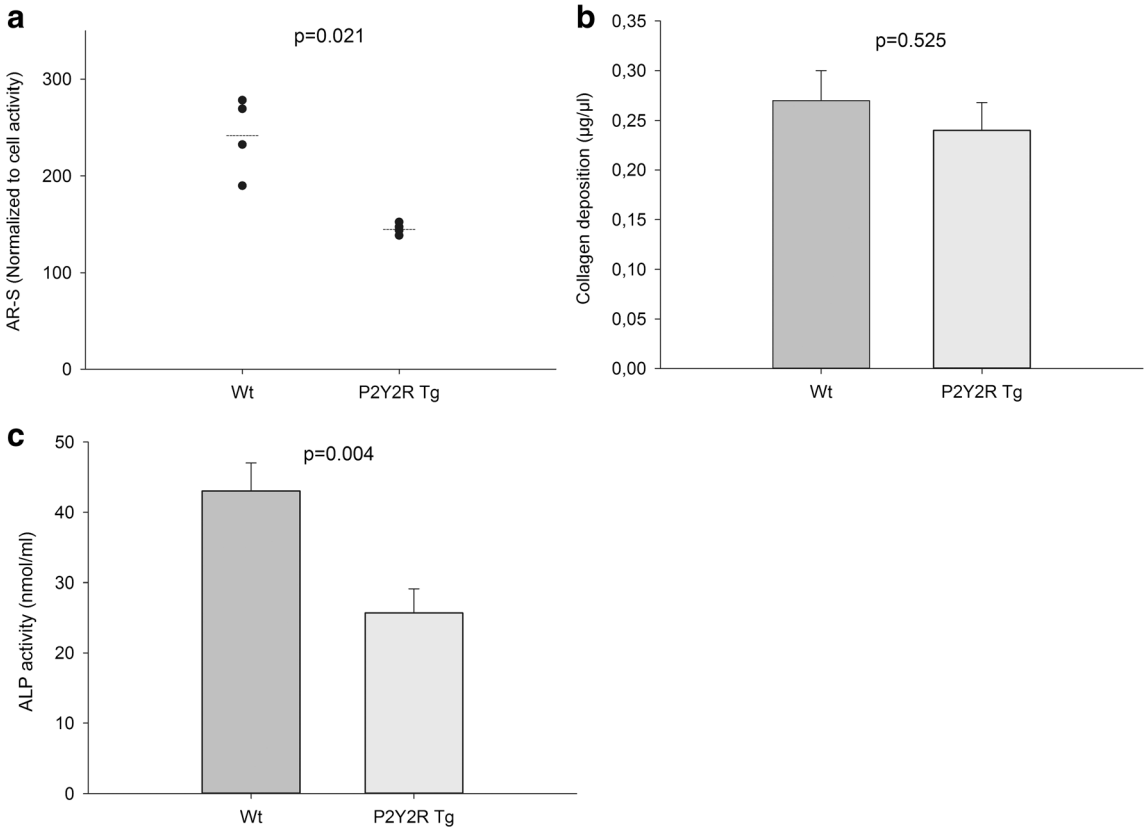

Fig. 5 **a** Bone nodule formation in osteoblast cultures stained with Alizarin Red (AR-S). **b** Production of fibrillary collagen in osteoblast cultures measured by Sirius Red stain. **c** Alkaline phosphatase (ALP) activity measured as percentage of total protein content in cell lysates. AR-S data are presented as individual experiments (mean of four replicates), mean (—) and *p* value from Mann-Whitney *U* test ($n = 4$). Collagen and ALP data are presented as mean ± SEM and *p* value from *t* test ($n = 10$)

tendency towards reduced resorption by osteoclasts from P2Y2R-Tg rats. There have been only limited reports on the effect of P2Y2R signaling in osteoclasts, and P2Y2R has been suggested to function as an off-switch of the osteoblastic mineralization process [6, 9]. This is in line with our findings of increased endosteal O.Th in the proximal tibia. In addition, our data suggest that P2Y2R signaling is able to modulate osteoclast formation and activity.

Dynamic histomorphometry showed less active mineralizing surfaces (MS/BS) in P2Y2R-Tg rats, but increased MAR. This could suggest fewer but more active osteoblasts. In support of this, we found no change in the serum markers of bone formation, PINP, and osteocalcin, which are both products from matrix formation. However, ALP activity in serum was significantly reduced in P2Y2R-Tg rats, which could reflect a decrease in the number of active osteoblasts, also apparent by the reduction in MS/BS. The effect on osteoblasts could be a direct effect of changes in P2Y2R signaling in these cells but could also be an indirect effect through changed P2Y2R signaling in the osteoclasts and thereby a change in the activation of osteoblasts following resorption. In order to assess the isolated effects of P2Y2R overexpression in osteoblasts, cells were isolated from P2Y2R-Tg and Wt rats. Calvarial osteoblasts from P2Y2R-Tg showed reduced formation of mineralized bone nodules after 7 days of culture, suggesting a direct effect of P2Y2R signaling on the osteoblasts. This was further supported by a reduction in ALP activity in the osteoblast cultures as well.

Orriss et al. showed that ATP and UTP stimulation of primary rat osteoblast cultures inhibited mineralization, accompanied by decreased ALP activity. This was suggested to be the result of P2Y2R activation, although inhibition of mineralization by pyrophosphate formed from ATP and UTP degradation is also a possibility [6, 7]. These findings are in agreement with the reduced ALP activity and mineralization seen in the primary osteoblasts from P2Y2R-overexpressing rats in our study. In a recent study, however, ATP and UTP were shown to increase mineralization and ALP activity in primary rat osteoblasts. Along with this, an increase in expression of BMP4 and BMP5, proteins involved in regulation of bone matrix formation, was seen upon stimulation with ATP and UTP [8]. Furthermore, Xing et al. showed that primary osteoblasts from P2Y2R KO mice formed less mineralized nodules and had lower ALP activity compared to osteoblasts from Wt mice [14].

Strikingly, histomorphometry showed a 40% increase in the thickness of the osteoid layer of the endocortical zones in the proximal part of the tibia in P2Y2R-Tg rats. These zones were close to the epiphysis and might be related to the increased bone length. In contrast, no osteoid was detected in the midshaft of the tibia. Thus, the increased bone length and the increased osteoid-forming activity might indicate an important role for P2Y2R in the regulation of longitudinal bone growth. Moreover, the increase in osteoid thickness was not reflected in increased cortical bone thickness.

Orriss et al. reported that 2-month-old male P2Y2R KO mice display a 17% increase in tibial BMC and a 9% increase in femoral BMC compared to Wt mice, supporting that P2Y2R activation inhibits mineralization [7], whereas Xing et al. reported contrasting results on the bone phenotype in P2Y2R KO in a recent study [14]. They found that both 8- and 17-week-old male P2Y2 KO mice have decreased trabecular BV/TV and Tb.Th. Corresponding changes in cortical bone appeared only after 17 weeks, while both trabecular and cortical BMD remained unchanged. Ultimate force and stiffness of cortical bone was decreased after 17 weeks, but not after 8 weeks [14]. The decrease in mechanical properties due to the lack of P2Y2R expression is in agreement with the increase in mechanical properties upon increased P2Y2R expression in our study. This also suggests that cortical changes might appear at a later stage in our model since mice and rats are considered skeletally mature at different ages (4 vs. 6 months of age, respectively) and could explain that we only see changes of mechanical properties of the femoral neck, which is rich in trabecular bone and not the cortical midshaft. It would be highly relevant to investigate the effect of P2Y2R overexpression in skeletally mature rats of at least 6 months of age, since the involvement of the receptor in bone modeling (growth) and bone remodeling might differ.

Data from transgenic models should always be interpreted with some caution. One limitation of the transgenic model in our study is that the actual insertion site(s) of the transgene and the number of insertion sites are currently unknown. As the transgene was inserted randomly using a lentiviral vector, there is a possibility that the insertion has disrupted another functional gene at one or more sites, contributing to the transgenic phenotype independent of P2Y2R. Furthermore, Agca et al. described that P2Y2R-Tg rats display signs of both nephropathy and inflammation [20], both of which can result in a changed bone turnover independent of P2Y2R signaling. The severity of these conditions was, however, reported to increase with age, and should therefore be minimized since the rats used in our study were only 3 months old. This should be considered and monitored if older animals were used to study the effect on skeletally mature animals. Another concern with this model could be that it does not reflect the true role of the receptor. In purinergic signaling, the receptor levels might not be the rate limiting factor. Thus, normal physiologic receptor levels might be sufficient for bone cell function, but with the ligand concentration being the rate limiting step. This could be investigated by stimulating the bone cell cultures with different concentrations of nucleotides/ligands to assess the effects of increased purinergic signaling on the bone-related end points used in this study.

In the clinical setting, studies suggest that the role of P2Y2R in regulation of bone turnover is of significance as

well. Several non-synonymous SNPs have been identified within the P2Y2R gene. Wesselius et al. reported that women with the Leu46Pro SNP had higher BMD compared to women carrying the Wt allele in a cohort of fracture patients [18]. Unfortunately, the effect on receptor function of this SNP has not yet been identified. In a Danish cohort study of postmenopausal women, the Arg312Ser SNP was shown to be associated with increased BMD and decreased rates of bone loss [19]. This SNP has been suggested to result in gain of function of P2Y2R. The P2Y2R genotype could therefore potentially serve as a prognostic marker for bone disease.

In conclusion, our study suggests that P2Y2R is involved in the regulation of bone turnover, due to its effects on both osteoblasts and osteoclasts, and that these effects might be very relevant in the regulation of bone growth in the young skeleton.

Acknowledgements This work was partially supported by the start-up funds from University of Missouri, National Institute of Health (grant no. P40 OD011062) and by the European Commission under the 7th Framework Programme (proposal no. 202231) performed as a collaborative project among the members of the ATPBone Consortium (Copenhagen University, University College London, University of Maastricht, University of Ferrara, University of Liverpool, University of Sheffield, and Université Libre de Bruxelles), and is a substudy under the main study "Fighting osteoporosis by blocking nucleotides: purinergic signalling in bone formation and homeostasis."

Author contributions Concept and design of the study: YA, NRJ, CA, AG. Conducting experiments: CA, YA, LSK, NW. Acquiring data: CA, YA, NRJ, SP, ME, AA, LSK, NW, AG, JEBJ. Analyzing data: NRJ, YA, CA, ME, SP, LSK, NW, AA, AG. Providing reagents and animal model: YA, CA. Writing, critically reviewing and approving the manuscript: NRJ, YA, CA, ME, SP, LSK, NW, AA, AG, JEBJ.

Compliance with ethical standards

Ethical approval All applicable international, national, and/or institutional guidelines for the care and use of animals were followed. All procedures performed in studies involving animals were in accordance with the ethical standards of the institution at which the studies were conducted.

Conflict of interest Maria Ellegaard declares that she has no conflict of interest.

Cansu Agca declares that she has no conflict of interest.
Solveig Petersen declares that she has no conflict of interest.
Ankita Agrawal declares that she has no conflict of interest.
Lars Schack Kruse declares that he has no conflict of interest.
Ning Wang declares that he/she has no conflict of interest.
Alison Gartland declares that she has no conflict of interest.
Jens-Erik Beck Jensen declares that he has no conflict of interest.
Niklas Rye Jørgensen declares that he has no conflict of interest.
Yuksel Agca declares that he has no conflict of interest.

References

1. Ralevic V, Burnstock G (1998) Receptors for purines and pyrimidines. Pharmacol Rev 50:413–492
2. Burnstock G, Arnett TR, Orriss IR (2013) Purinergic signalling in the musculoskeletal system. Purinergic Signal 9:541–572
3. James G, Butt AM (2001) P2X and P2Y purinoreceptors mediate ATP-evoked calcium signalling in optic nerve glia in situ. Cell Calcium 30:251–259
4. Bowler WB, Dixon CJ, Halleux C, Maier R, Bilbe G, Fraser WD, Gallagher JA, Hipskind RA (1999) Signaling in human osteoblasts by extracellular nucleotides. Their weak induction of the c-fos proto-oncogene via Ca2+ mobilization is strongly potentiated by a parathyroid hormone/cAMP-dependent protein kinase pathway independently of mitogen-activated protein kinase. J Biol Chem 274: 14315–14324
5. Schofl C, Cuthbertson KS, Walsh CA, Mayne C, Cobbold P, von-zur Mühlen A, Hesch RD, Gallagher JA (1992) Evidence for P2-purinoceptors on human osteoblast-like cells. J Bone Miner Res 7: 485–491
6. Orriss IR, Knight GE, Ranasinghe S, Burnstock G, Arnett TR (2006) Osteoblast responses to nucleotides increase during differentiation. Bone 39:300–309
7. Orriss IR, Utting JC, Brandao-Burch A, Colston K, Grubb BR, Burnstock G, Arnett TR (2007) Extracellular nucleotides block bone mineralization in vitro: evidence for dual inhibitory mechanisms involving both P2Y2 receptors and pyrophosphate. Endocrinology 148:4208–4216
8. Ayala-Pena VB, Scolaro LA, Santillan GE (2013) ATP and UTP stimulate bone morphogenetic protein-2,-4 and -5 gene expression and mineralization by rat primary osteoblasts involving PI3K/AKT pathway. Exp Cell Res 319:2028–2036
9. Bowler WB, Littlewood-Evans A, Bilbe G, Gallagher JA, Dixon CJ (1998) P2Y2 receptors are expressed by human osteoclasts of giant cell tumor but do not mediate ATP-induced bone resorption. Bone 22:195–200
10. Jorgensen NR, Geist ST, Civitelli R, Steinberg TH (1997) ATP- and gap junction-dependent intercellular calcium signaling in osteoblastic cells. J Cell Biol 139:497–506
11. Jorgensen NR, Henriksen Z, Sorensen OH, Eriksen EF, Civitelli R, Steinberg TH (2002) Intercellular calcium signaling occurs between human osteoblasts and osteoclasts and requires activation of osteoclast P2X7 receptors. J Biol Chem 277:7574–7580
12. Jorgensen NR, Henriksen Z, Brot C, Eriksen EF, Sorensen OH, Civitelli R, Steinberg TH (2000) Human osteoblastic cells propagate intercellular calcium signals by two different mechanisms. J Bone Miner Res 15:1024–1032
13. Gardinier J, Yang W, Madden GR, Kronbergs A, Gangadharan V, Adams E, Czymmek K, Duncan RL (2014) P2Y2 receptors regulate osteoblast mechanosensitivity during fluid flow. Am J Phys Cell Phys 306:C1058–C1067
14. Xing Y, Gu Y, Bresnahan JJ, Paul EM, Donahue HJ, You J (2014) The roles of P2Y2 purinergic receptors in osteoblasts and mechanotransduction. PLoS One 9:e108417
15. Buscher R, Hoerning A, Patel HH, Zhang S, Arthur DB, Grasemann H, Ratjen F, Insel PA (2006) P2Y2 receptor polymorphisms and haplotypes in cystic fibrosis and their impact on Ca2+ influx. Pharmacogenet Genomics 16:199–205
16. Dasari VR, Sandhu AK, Mills DC, Athwal RS, Kunapuli SP (1996) Mapping of the P2U purinergic receptor gene to human chromosome 11q 13.5–14.1. Somat Cell Mol Genet 22:75–79
17. Janssens R, Paindavoine P, Parmentier M, Boeynaems JM (1999) Human P2Y2 receptor polymorphism: identification and pharmacological characterization of two allelic variants. Br J Pharmacol 127:709–716
18. Wesselius A, Bours MJ, Henriksen Z, Syberg S, Petersen S, Schwarz P, Jorgensen NR, van Helden S, Dagnelie PC (2013) Association of P2Y(2) receptor SNPs with bone mineral density

and osteoporosis risk in a cohort of Dutch fracture patients. Purinergic Signal 9:41–49
19. Wesselius A, Bours MJ, Agrawal A, Gartland A, Dagnelie PC, Schwarz P, Jorgensen NR (2011) Role of purinergic receptor polymorphisms in human bone. Front Biosci (Landmark Ed) 16:2572–2585
20. Agca C, Seye C, Kashuba Benson CM, Rikka S, Chan AW, Weisman GA, Agca Y (2009) Development of a novel transgenic rat overexpressing the P2Y(2) nucleotide receptor using a lentiviral vector. J Vasc Res 46:447–458
21. Ellegaard M, Kringelbach T, Syberg S, Petersen S, Beck Jensen JE, Bruel A, Jorgensen NR, Schwarz P (2013) The effect of PTH(1–34) on fracture healing during different loading conditions. J Bone Miner Res 28:2145–2155
22. Syberg S, Schwarz P, Petersen S, Steinberg TH, Jensen JE, Teilmann J, Jorgensen NR (2012) Association between P2X7 receptor polymorphisms and bone status in mice. J Osteoporos 2012: 637986
23. Orriss IR, Taylor SE, Arnett TR (2012) Rat osteoblast cultures. Methods Mol Biol 816:31–41
24. Dahl M, Syberg S, Jorgensen NR, Pinholt EM (2013) Adipose derived mesenchymal stem cells—their osteogenicity and osteoblast in vitro mineralization on titanium granule carriers. J Craniomaxillofac Surg 41:e213–e220
25. Goodyear SR, Gibson IR, Skakle JM, Wells RP, Aspden RM (2009) A comparison of cortical and trabecular bone from C57 Black 6 mice using Raman spectroscopy. Bone 44:899–907